

pubs.acs.org/JACS Article

# Formation of Red Elemental Selenium from Seleniferous Oxyanions: Deoxygenation by a Homogeneous Iron Catalyst

Kelly L. Gullett, Courtney L. Ford, Ian J. Garvey, Tabitha J. Miller, Clare A. Leahy, Lisa N. Awaitey, Daniel M. Hofmann, Toby J. Woods, and Alison R. Fout\*



Cite This: J. Am. Chem. Soc. 2023, 145, 20868-20873



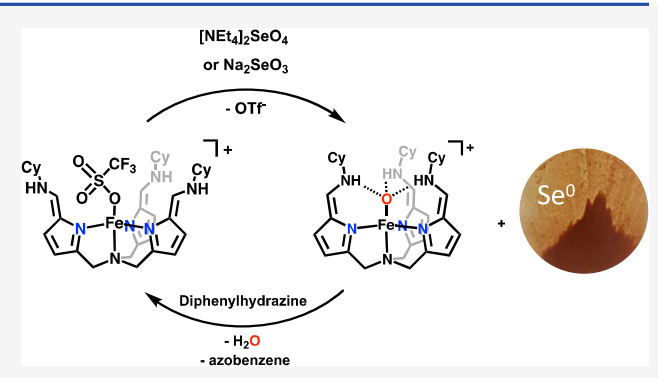
**ACCESS** 

Metrics & More

Article Recommendations

Supporting Information

ABSTRACT: Seleniferous oxyanions are groundwater contaminants from both anthropogenic and natural sources, while pure amorphous selenium nanoparticles have a variety of industrial applications. Biology can achieve the multicomponent 6 e<sup>-</sup>/8 H<sup>+</sup> reduction of selenate to amorphous selenium using multiple metalloenzymes, like selenate and selenite reductase. Inspired by biology, we developed a new homogeneous system that can generate pure elemental selenium with no caustic waste. The stoichiometric reductions of selenate, selenite, and selenium dioxide with an iron(II) complex produced an iron(III)-oxo and red elemental selenium, the latter of which has been characterized by a variety of spectroscopic techniques. The catalytic reduction of SeO<sub>4</sub><sup>2-</sup> and SeO<sub>3</sub><sup>2-</sup> directly to amorphous Se and isolated as Se=PPh<sub>3</sub> is reported with a turnover number of 12 and 7, respectively.



## **■ INTRODUCTION**

Selenium-containing oxyanions, selenate (SeO<sub>4</sub><sup>2-</sup>) and selenite (SeO<sub>3</sub><sup>2-</sup>), are the highly water-soluble and mobile oxidized forms of elemental selenium, originating in the global water cycle from both natural and anthropogenic sources. 1,2 For example, the combination of selenium-rich soil and industrial agricultural practices in California led to the 1989 discovery of the first organism, T. Selenatus, capable of withstanding the resulting toxic concentrations of aqueous seleniferous oxyanions in the San Joaquin Valley.<sup>3–5</sup> The enzyme responsible for the reduction of  $SeO_4^{2-}$  to  $SeO_3^{2-}$  within T. Selenatus is a periplasmic molybdenum-containing metalloenzyme named selenate reductase, which catalyzes the reduction via a proposed oxygen atom transfer mechanism (Figure 1A).<sup>6,7</sup> SeO<sub>3</sub><sup>2-</sup> is then metabolized to amorphous selenium (a-Se) through multiple biochemical mechanisms including dissimilatory reduction and detoxification pathways (Figure 1A) or can be further reduced to selenide (Se<sup>2-</sup>) via assimilatory pathways or methylation processes.<sup>4,8</sup> A variety of reductases (nitrite, sulfite, glutathione, selenite reductases, etc.) can all produce a-Se from aqueous SeO<sub>3</sub><sup>2-4,8-10</sup> Amorphous Se produced from these biochemical pathways has been well characterized by spectroscopic methods including demonstrations where the bacterial mixtures take on selenium's distinct red-orange color.11,12

Despite the numerous biochemical pathways capable of carrying out the 4-electron reduction of SeO<sub>3</sub><sup>2-</sup> to Se<sup>0</sup>, there is a surprising lack of homogeneous catalysts capable of

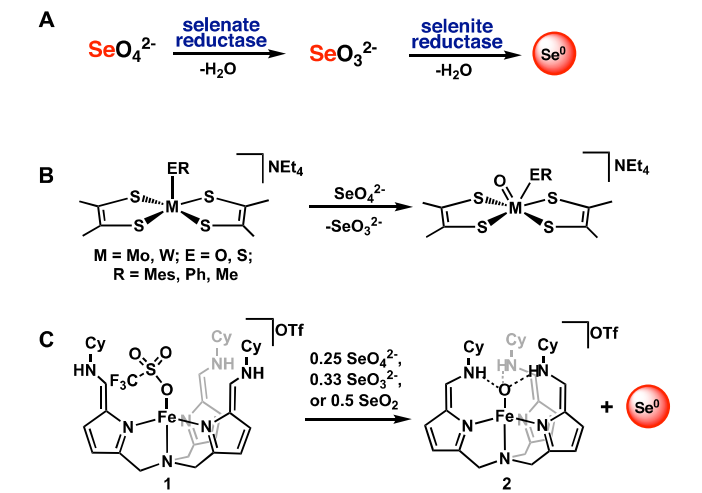


**Figure 1.** Selected examples of selenium oxyanion reduction. (A) Biological seleniferous oxyanion reduction. (B) Stoichiometric reduction of  $SeO_4^{\ 2^-}$  to  $SeO_3^{\ 2^-}$  by Holm and co-workers. (C) This work.

Received: June 7, 2023 Published: September 15, 2023





generating a-Se from seleniferous oxyanions. Zero-valent iron (ZVI) nanoparticles have been demonstrated to reduce Seoxyanions and encapsulate the selenide and selenium produced. 13,14 Holm and co-workers designed a model complex of selenate reductase utilizing a Mo<sup>IV</sup>-(bis)dithiolene system,  $[Mo(OR)(S_2C_2(Me_2)_2]^-$  (R = Me or Ph). Addition of SeO<sub>4</sub><sup>2-</sup> to the Mo<sup>IV</sup> complexes resulted in the formation of a molybdenum<sup>VI</sup>-oxo via an oxygen atom transfer reaction but, similarly to selenate reductase, the molybdenum species was unable to further reduce SeO<sub>3</sub><sup>2-</sup> to Se<sup>0</sup> (Figure 1B). Inspired by the structural similarities found in the active sites of (per)chlorate reductase, 16 respiratory nitrate reductase, 17 and selenate reductase<sup>7</sup> and the successes our non-heme iron system,  $[N(afa^{Cy})_3FeOTf]OTf$  (1),  $^{18-21}$  has achieved at replicating this reactivity, we sought to expand the scope of reducible oxyanions in our system toward seleniferous oxyanions. Further, we hypothesized that by creating a homogeneous system capable of reducing the seleniferous oxyanions, the reduction would result in the formation of pure selenium, unhindered with iron contaminants (in the case of ZVI species) or needing to be excreted from the organism (in biological reduction). Further, this homogeneous reaction would be less energy-intensive and limit caustic waste production as approximately 90% of all elemental selenium is produced from the separation of byproducts during electrolytic copper refining.<sup>2,6</sup> Here, we report the catalytic reduction of SeO<sub>4</sub><sup>2-</sup> and SeO<sub>3</sub><sup>2-</sup> directly to a-Se with 1 to produce an Fe<sup>III</sup>oxo,  $\frac{7}{2}$  [N(afa<sup>Cy</sup>)<sub>3</sub>FeO]OTf, (2), <sup>18</sup> and a-Se (Figure 1C).

### RESULTS AND DISCUSSION

Stoichiometric Reduction of SeO<sub>4</sub><sup>2-</sup> and SeO<sub>3</sub><sup>2-</sup>. To investigate the reduction of seleniferous oxyanions, 4 equivalents (equiv) of 1 were added to tetraethylammonium selenate ([NEt<sub>4</sub>]<sub>2</sub>SeO<sub>4</sub>), a salt readily soluble in organic solvents, specifically acetonitrile (MeCN). After 48 h, the solution had taken on a brown hue, the color of the terminal Fe<sup>III</sup>-oxo, 2, the expected product of oxyanion reduction (Figure 1C). Analysis of the crude reaction mixture by <sup>1</sup>H NMR spectroscopy showed unreacted starting material 1 and a small quantity of 2 (Figure S12). We initially considered the low production of 2 was caused by 1 accomplishing only one deoxygenation step, akin to Holm and co-workers, rather than reducing SeO<sub>4</sub><sup>2-1</sup> to a-Se (vide supra). To evaluate this hypothesis, we turned to the reduction of sodium selenite (Na<sub>2</sub>SeO<sub>3</sub>) by 1, a reduction that could not be achieved by the Holm system. Methanol (MeOH) was added to the reaction mixture to increase the solubility of Na<sub>2</sub>SeO<sub>3</sub>. Upon addition, the solution immediately changed color from yellow to orange, and within 1 hour, the solution began to turn brown. Over the course of 24 hours, the solution became chocolate brown in color and the formation of a red precipitate was observed. Analysis of the crude reaction mixture by <sup>1</sup>H NMR spectroscopy revealed a mixture of 2 and unreacted 1 (Figure S13). <sup>77</sup>Se NMR spectroscopy was attempted to identify the Se intermediates or products formed in the reaction. Unfortunately, due to the signal quenching caused by the paramagnetic iron center, no resonances could be detected in the <sup>77</sup>Se NMR

Characterization of Red Elemental Selenium. Given the colloidal and insoluble nature of the red precipitate (*vide supra*), we hypothesized that a-Se was generated during the reduction of Na<sub>2</sub>SeO<sub>3</sub>. The red precipitate was characterized through reactivity and spectroscopic studies (Figure 2, and see

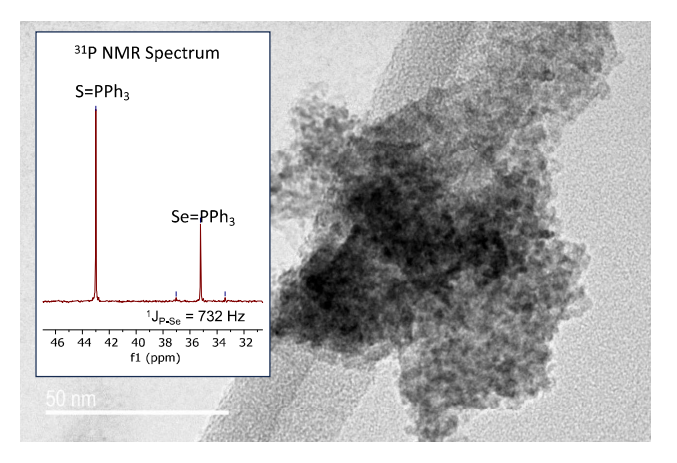


Figure 2. Inset:  $^{31}P$  NMR spectrum showing the isolation of Se = PPh<sub>3</sub> referenced to S = PPh<sub>3</sub>. TEM image of the <10 nm isolated amorphous selenium.

the SI) to confirm this hypothesis. The reactivity of Se<sup>0</sup> with phosphines is a well-characterized and quantitative technique used to determine the sigma-donating and pi-accepting abilities of phosphines via the chemical shifts and coupling constants of the resulting phosphine selenide complexes using <sup>31</sup>P NMR spectroscopy.<sup>23</sup> Addition of the isolated red precipitate to a solution of triphenylphosphine (PPh3) resulted in gradual dissolution over the course of 4 h and the successful synthesis of triphenylphosphine selenide (Se = PPh<sub>3</sub>) as confirmed by the <sup>31</sup>P NMR resonance at 35.22 ppm, including the expected Se satellites  ${}^{1}J_{P-Se} = 732 \text{ Hz}$  (Figure 2, inset). Furthermore, this was consistent with independently synthesized Se = PPh<sub>3</sub> from Se<sup>0</sup> and PPh<sub>3</sub> (Figure S7). Transmission electron microscopy (TEM) images were obtained of the isolated red solid, describing the formation of small (<10 nm) particles (Figure 2). UV-visible spectroscopy of a suspension of the isolated solids in water confirmed the Se<sup>0</sup> as red selenium rather than black or gray selenium (Figure S11). Furthermore, the resulting pattern obtained from powder X-ray diffraction studies was consistent with the isolated material being amorphous in nature (Figure S10). To ensure that the reduction of SeO<sub>3</sub><sup>2-</sup> to a-Se proceeded homogeneously, it was essential to confirm that the a-Se produced was free of iron contamination, which was accomplished using thermal neutron irradiation studies. Qualitative analysis of the produced  $\gamma$  ray spectrum confirmed the presence of only selenium atoms, showing no evidence of iron contamination (Tables S2-S4). The formation of pure amorphous red selenium unencumbered by iron contamination shows the deoxygenation power of our iron catalyst. The combination of metal ion, weak ligand field provided by the pyrrole-based ligand, and the secondary coordination sphere effects allow for the reduction of Se<sup>IV</sup> to Se<sup>0</sup>, but will not further reduce Se<sup>0</sup> to form an iron selenide species, as displayed in a related system developed by Borovik.<sup>24</sup>

**Investigation of Methanol Dependency.** The rate of oxyanion reduction by 1 is highly dependent on the coordinating ability of the reaction solvent, as determined in previous work with perchlorate reduction. The immediate color change from yellow to orange noted upon the addition of MeOH to the reaction mixture suggested that MeOH was interacting with 1 (Figure 3A), and subsequently leading to increased reactivity toward seleniferous oxyanion reduction. Analysis of 1, after exposure to a 3:1 mixture of MeCN:MeOH,

[NEt<sub>4</sub>]<sub>2</sub>SeO<sub>4</sub>

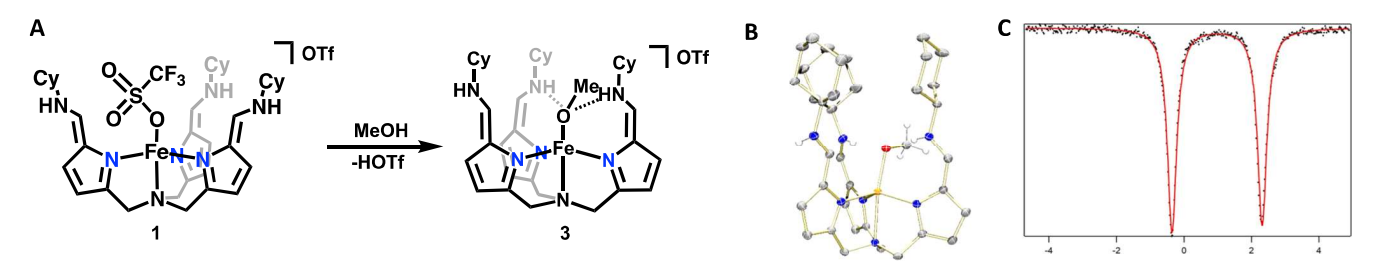


Figure 3. (A) Reaction of 1 with MeOH to produce 3. (B) Molecular structure of 3 shown with 50% probability ellipsoids. For clarity, only the MeOH and amine-bound hydrogen atoms are shown and the outer-sphere triflate anion has been omitted. (C) Zero-field  $^{57}$ Fe Mössbauer spectrum of [N(afa<sup>Cy</sup>)<sub>3</sub>Fe(OMe)]OTf collected at 90 K. Isomer shift and quadrupole splitting are referenced to Fe foil at room temperature. Isomer shift ( $\delta$ ) = 0.98 mm/s and quadrupole splitting ( $\Delta$ EQ) = 2.67 mm/s.

12

H<sub>2</sub>SeO<sub>3</sub>

by <sup>1</sup>H NMR spectroscopy in MeCN-d<sub>3</sub> showed no change in the paramagnetic region (Figure S2). Conversely, the spectrum obtained in MeOH-d4 revealed the formation of a new paramagnetic complex. Reaction of 1 and freshly synthesized NaOMe in MeCN resulted in the same paramagnetic NMR spectrum, giving insights that this might be a bound methoxide instead of methanol. Orange crystals suitable for X-ray diffraction were grown from vapor diffusion of diethyl ether (Et<sub>2</sub>O) into a concentrated solution of 1 in a 2:1 MeCN/ MeOH mixture. The structure confirmed the formation of a new Fe complex with a methoxide bound in the axial position of the iron center (Figure 3B). The crystal structure revealed the presence of only one outer-sphere triflate counter anion and a distorted trigonal bipyramidal geometry  $(\tau^5 = 0.5)^{25}$ about the iron center. A comparison of Fe-O bond distances in 3 to previously reported complexes utilizing our ligand framework revealed that the Fe-O bond distance in 3 (2.02(5) Å) is more similar to that of an anionically bound hydroxide moiety (2.03(4) Å) found in  $[N(pi^{Cy})(afa^{Cy})_2Fe^{-1}]$ (OH)]OTf rather than a datively bound water molecule (2.08(0) Å) found in  $K[N(pi^{Cy})_3Fe(H_2O)]$ . The pyrrolebased tripodal ligand has flexible coordination modes that can lead to oxidation state ambiguity, either anionic coordination via a pyrrole-imine (pi) arm or dative coordination via an azafulvene amine (afa) arm, which is assigned based on the presence of hydrogen atoms in the secondary coordination sphere and IR spectroscopy.<sup>26</sup> The three secondary coordination sphere amine-bound hydrogen atoms were allowed to freely refine and could be found in the difference map. Additionally, the C=N stretching mode of 3 was found at 1650 cm<sup>-1</sup>, confirming the assignment of three datively coordinating afa arms of the ligand framework. Taken together, the data corresponds to 3 being an iron(II)-methoxide complex,  $[N(afa^{Cy})_3Fe(OMe)]OTf$ .

Characterization of the electronic structure of 3 further confirmed the presence of an Fe<sup>II</sup> metal center. Magnetic susceptibility data revealed a room-temperature  $\chi T$  value of 5.41(9)  $\mu$ B, which falls in the range of reported S = 5/2 Fe<sup>II</sup> complexes in our ligand framework. The assignment of highspin Fe<sup>II</sup> was corroborated by <sup>57</sup>Fe Mössbauer spectroscopy, which revealed a quadrupole doublet with an isomer shift ( $\delta$ ) of 0.98 mm/s and large quadrupole splitting ( $\Delta$ EQ) of 2.67 mm/s (Figure 3C).

In Situ Quantification of Red Elemental Selenium. With the identity of the red precipitate confirmed and a more thorough understanding of how methanol interacts with 1, we then looked to quantify the a-Se generated during the reduction of the oxyanions (Table 1). Due to the increased reactivity of 1 toward Na<sub>2</sub>SeO<sub>3</sub> compared to [NEt<sub>4</sub>]<sub>2</sub>SeO<sub>4</sub>,

Table 1. Stoichiometric Reduction of Seleniferous Oxyanions in the Presence of Varying O<sub>2</sub> ppm<sup>a</sup>

|       | Na <sub>2</sub> SeO <sub>3</sub>   | SePPh <sub>3</sub> |                             |             |                      |                     |
|-------|------------------------------------|--------------------|-----------------------------|-------------|----------------------|---------------------|
|       | SeO <sub>2</sub>                   |                    | - 2<br>- O=PPh <sub>3</sub> |             |                      |                     |
| entry | seleniferous<br>species            | <i>T</i><br>(°C)   | O <sub>2</sub><br>(ppm)     | time<br>(h) | $Se = PPh_3$ (equiv) | $O = PPh_3$ (equiv) |
| 1     | $Na_2SeO_3$                        | 23                 | 15                          | 24          | 0.96                 | 0.91                |
| 2     | $Na_2SeO_3$                        | 23                 | 10                          | 24          | 0.79                 | 0.54                |
| 3     | $Na_2SeO_3$                        | 23                 | 1.0≥                        | 24          | 0.55                 | trace               |
| 4     | $Na_2SeO_3$                        | 23                 | 1.0≥                        | 48          | 0.68                 | 0.0                 |
| 5     | $Na_2SeO_3$                        | 70                 | 1.7                         | 24          | 0.90                 | 0.18                |
| 6     | $[\mathrm{NEt_4}]_2\mathrm{SeO_4}$ | 23                 | 15                          | 24          | 0.40                 | 0.19                |
| 7     | $[NEt_4]_2SeO_4$                   | 23                 | 1.0≥                        | 48          | 0.31                 | trace               |
| 8     | $[\mathrm{NEt_4}]_2\mathrm{SeO_4}$ | 70                 | 15                          | 24          | 0.91                 | 0.65                |
| 9     | $[\mathrm{NEt_4}]_2\mathrm{SeO_4}$ | 70                 | 1.0≥                        | 24          | 0.47                 | trace               |
| 10    | $SeO_2$                            | 23                 | 1.0≥                        | 48          | 0.55                 | 0.0                 |
| 11    | $SeO_2$                            | 70                 | 1.0≥                        | 24          | 0.76                 | 0.0                 |

4, 3, or 2 equiv of 1

xs PPh<sub>3</sub>

3:1 MeCN:MeOH

"Number of equivalents of **1** equals the number of oxygens in the seleniferous oxyanion. "Half an equivalent of S = PPh<sub>3</sub> was utilized for quantification (2.0 equivalents expected).

1.0≥

23

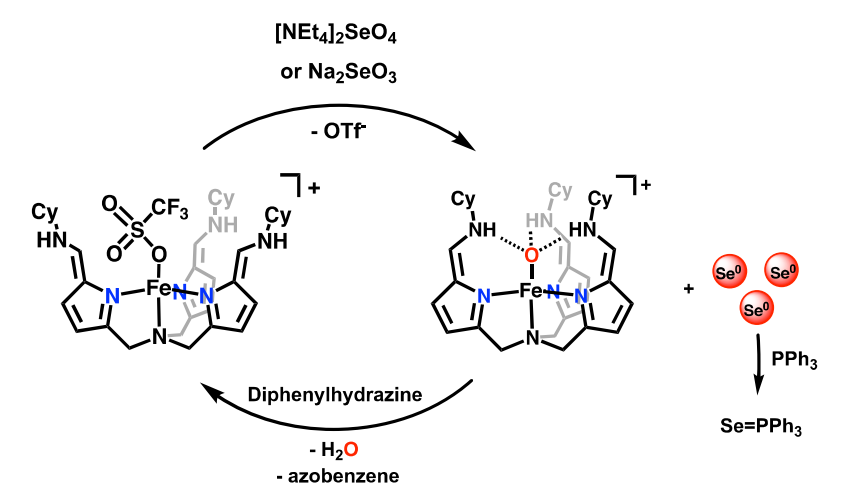
24

 $1.54^{b}$ 

0.0

optimization of quantification methods for a-Se was first established using the stoichiometric reduction of  $Na_2SeO_3$ . Quantification of the produced a-Se through isolation was not reliable due to the colloidal nature of the product and its tendency to adhere to the wall of the reaction vessels (Figure S39). Addition of PPh<sub>3</sub> to the reaction mixture to enable the *in situ* quantification of a-Se; production of Se = PPh<sub>3</sub> was monitored using <sup>31</sup>P NMR spectroscopy and quantified by the addition of an internal standard with similar solubility in organic solvents, triphenylphosphine sulfide (S = PPh<sub>3</sub>). Allowing the stoichiometric reduction of  $SeO_3^{2-}$  to run for 24 h in a MeCN/MeOH mixture in the presence of PPh<sub>3</sub> afforded Se = PPh<sub>3</sub> in 96% yield and triphenylphosphine oxide (O = PPh<sub>3</sub>) (Table 1, entry 1).

The observation of  $O = PPh_3$  suggested  $PPh_3$  was contributing to the reduction and deoxygenation of  $Na_2SeO_3$ , rather than the reduction occurring solely at the  $Fe^{II}$  center. Control reactions of  $Na_2SeO_3$  with  $PPh_3$  in the absence of 1 yielded no  $Se = PPh_3$  or  $O = PPh_3$ . Further control reactions of 1 and 2 with  $PPh_3$ , yielded no formation of  $O = PPh_3$ . Upon multiple repetitions of the experiments over the course of several months, we concluded that the formation of  $O = PPh_3$  and the yield of  $Se = PPh_3$  were correlated to trace amounts of oxygen present in the glovebox  $N_2$  atmosphere. Indeed, higher



| Reagent                                           | Amount of Se=PPh <sub>3</sub> produced (equiv) | TON |
|---------------------------------------------------|------------------------------------------------|-----|
| [NEt <sub>4</sub> ] <sub>2</sub> SeO <sub>4</sub> | 3.03                                           | 12  |
| Na <sub>2</sub> SeO <sub>3</sub>                  | 2.44                                           | 7   |



Figure 4. (Left) Catalytic reduction of selenate and selenite. (Right) Table describing TON and depiction of isolated red a-Se.

levels of adventitious  $O_2$ , 10–15 ppm (Table 1, entries 1 and 2), increased the production of  $O = PPh_3$  and  $Se = PPh_3$ , while a glovebox atmosphere containing less than 1.0 ppm of O<sub>2</sub> produced no O = PPh3 and a significantly lower yield of Se = PPh<sub>3</sub> (see Table 1, entry 3). This dependence on O<sub>2</sub> is also observed in the biological systems whereby the enzyme can function both aerobically and anaerobically to produce a-Se. 27,28 Once this observation was made, both room-temperature and elevated-temperature experiments were completed in a glovebox atmosphere containing low levels of O2 to achieve a reliable quantification of the produced a-Se in the stoichiometric reduction of Na<sub>2</sub>SeO<sub>3</sub> (Table 1, entries 4 and 5). These results indicated that 1 successfully reduced Na<sub>2</sub>SeO<sub>3</sub> to a-Se in 90% yield when heated to 70 °C for 24 h (Table 1, entry 5). Unlike 1, the stoichiometric reduction of Na<sub>2</sub>SeO<sub>3</sub> with 3 equiv of 3 proceeded in the absence of MeOH (Table S5, entries 3 and 8). Though low yielding, the production of Se = PPh<sub>3</sub> indicates that 3 is likely more reactive toward a suspension of Na<sub>2</sub>SeO<sub>3</sub> compared to that of 1. Due to the lower solubility of crystalline 3 in acetonitrile, further reactions utilized MeOH in the solvent system to generate 3 in situ.

With a method of quantification established and conditions optimized the remaining stoichiometric reductions of [NEt<sub>4</sub>]<sub>2</sub>SeO<sub>4</sub>, selenium dioxide (SeO<sub>2</sub>), and selenious acid (H<sub>2</sub>SeO<sub>3</sub>) were achieved. The positive correlation between atmospheric  $O_2$  and yield of  $Se = PPh_3$  and  $O = PPh_3$  was also observed in the stoichiometric reduction of [NEt<sub>4</sub>]<sub>2</sub>SeO<sub>4</sub> (Table 1, entries 6–9). Further, as noted above in the initial stoichiometric reductions, the reduction of [NEt<sub>4</sub>]<sub>2</sub>SeO<sub>4</sub> gave a lower yield of both Se = PPh<sub>3</sub> and 2 compared to that of Na<sub>2</sub>SeO<sub>3</sub>. This trend is also observed in both heterogeneous and biological reductions of seleniferous oxyanions. <sup>4,13</sup> Finally, the reduction of SeO<sub>2</sub> was complicated due to unsurprising background reactivity between SeO2 and PPh3 leading to the formation of Se = PPh<sub>3</sub> and O = PPh<sub>3</sub> without the addition of a catalytic metal center. Unlike the seleniferous oxyanions, SeO<sub>2</sub> is commonly used as an oxidant in organic transformations.<sup>29,30</sup> Interestingly, the one-pot reduction of SeO<sub>2</sub> with 2 equiv of 1 in the presence of PPh3 in a glovebox atmosphere containing less than 1.0 ppm of  $O_2$  showed only the formation of Se =  $PPh_3$  (Table 1, entries 10–11). To further test the oxophilicity of our iron center and the ability to react with neutral selenium complexes, 1 was reacted with selenious acid (Table 1, entry 12). After 24 h at room temperature, the

conversion of selenious acid to a-Se was achieved in 77% yield with no  $O = PPh_3$  formed in the reaction. The reactivity of  $SeO_2$  and  $H_2SeO_3$  in the presence of  $PPh_3$  and 1 without the formation of  $O = PPh_3$  confirms that the deoxygenation step at the  $Fe^{II}$  center is quite facile, outcompeting  $PPh_3$ . These results further support that the formation of  $O = PPh_3$  is likely from atmospheric  $O_2$ .

Catalytic Reduction of  $SeO_3^{2-}$  and  $SeO_4^{2-}$ . The catalytic reduction of  $SeO_4^{2-}$  to a-Se and  $H_2O$  requires 6  $e^-/8$  H<sup>+</sup> and is achieved by multiple metalloenzymes in biological systems. As previously reported, **2** can be reduced to the reactive  $Fe^{II}$  complex *in situ* via the addition of a proton and electron source, 1,2-diphenylhydrazine (DPH), with concomitant formation of azobenzene and 1 equiv of water.  $^{19,20}$  We next tested the reactivity of both  $SeO_3^{2-}$  and  $SeO_4^{2-}$  toward DPH. Control reactions (Figures S33 and S34) of DPH with the various seleniferous oxyanions in MeCN at room temperature show no conversion of DPH to azobenzene with the oxyanions and minimal conversion with  $SeO_2$  and  $H_2SeO_3$ . Further, heating the oxyanions at 70 °C with DPH shows less than 2% conversion to azobenzene. Based on these control reactions, the catalytic reduction of  $Na_2SeO_3$  and  $[NEt_4]_2SeO_4$  was investigated.

A one-pot system including 1 equiv of 1, 4 equiv of [NEt<sub>4</sub>]<sub>2</sub>SeO<sub>4</sub>, 22 equiv of DPH, and 20 equiv of PPh<sub>3</sub> was stirred in a MeCN/MeOH mixture for 72 h at 70 °C. Analysis of the <sup>31</sup>P NMR spectrum showed the formation of 2.5 equiv of Se = PPh<sub>3</sub> and a TON of 10 (1.0 equiv of Se = PPh<sub>3</sub> corresponds to a turnover number (TON) of 4) (Table S7). Decreasing the catalyst loading from 25 to 20% and allowing the reduction to stir for 120 h at 70 °C increased the production of Se = PPh<sub>3</sub> to 3.03 equiv for a TON of 12 (Figure 4). In a reaction setup akin to [NEt<sub>4</sub>]<sub>2</sub>SeO<sub>4</sub>, the catalytic reduction of Na<sub>2</sub>SeO<sub>3</sub> was targeted. The one-pot system included 1 equiv of 1, 4 equiv of Na<sub>2</sub>SeO<sub>3</sub>, 18 equiv of DPH, and 12 equiv of PPh<sub>3</sub>, and stirred in a MeCN/MeOH mixture for 72 h at 70 °C. Analysis of the <sup>31</sup>P NMR spectrum showed the formation of 2.44 equivalents of Se = PPh<sub>3</sub> corresponding to a TON of 7.

## CONCLUSIONS

Herein, we described the reduction of selenate and selenite by  $[N(afa^{Cy})_3FeOTf]OTf$  to form an  $Fe^{III}$ -oxo complex and amorphous red elemental selenium. The catalytic reduction of

 ${\rm SeO_3}^{2-}$  and  ${\rm SeO_4}^{2-}$  to a-Se and  ${\rm H_2O}$  is described achieving a difficult multielectron/multiproton process with a single iron center. This catalytic sequence represents the conversion of a toxic waste stream to a usable product. This work represents a rare example of a single homogeneous catalyst capable of fully completing the reduction sequence of seleniferous oxyanions to form amorphous selenium. Characterization of the a-Se confirmed it was amorphous, red, <10 nm, and pure Se. The stochiometric reduction of selenium dioxide and selenious acid was also described.

## ASSOCIATED CONTENT

## Supporting Information

The Supporting Information is available free of charge at https://pubs.acs.org/doi/10.1021/jacs.3c05981.

Experimental details of the catalytic reactions and spectral details (PDF)

### **Accession Codes**

CCDC 2210259 contains the supplementary crystallographic data for this paper. These data can be obtained free of charge via <a href="https://www.ccdc.cam.ac.uk/data\_request/cif">www.ccdc.cam.ac.uk/data\_request/cif</a>, or by emailing data\_request@ccdc.cam.ac.uk, or by contacting The Cambridge Crystallographic Data Centre, 12 Union Road, Cambridge CB2 1EZ, UK; fax: +44 1223 336033.

Crystallographic details for compound 3 CCDC 2210259 contain the supplementary crystallographic data for this paper. These data can be obtained free of charge via www.ccdc.cam. ac.uk/data\_request/cif.

### AUTHOR INFORMATION

#### **Corresponding Author**

Alison R. Fout — Department of Chemistry, Texas A&M University, College Station, Texas 77843, United States; orcid.org/0000-0002-4669-5835; Email: fout@tamu.edu

#### **Authors**

- Kelly L. Gullett School of Chemical Sciences, University of Illinois at Urbana-Champaign, Urbana, Illinois 61802, United States
- Courtney L. Ford School of Chemical Sciences, University of Illinois at Urbana-Champaign, Urbana, Illinois 61802, United States; orcid.org/0000-0002-1509-4850
- Ian J. Garvey School of Chemical Sciences, University of Illinois at Urbana-Champaign, Urbana, Illinois 61802, United States
- Tabitha J. Miller School of Chemical Sciences, University of Illinois at Urbana-Champaign, Urbana, Illinois 61802, United States
- Clare A. Leahy School of Chemical Sciences, University of Illinois at Urbana-Champaign, Urbana, Illinois 61802, United States; Occid.org/0000-0001-5042-1418
- Lisa N. Awaitey Department of Chemistry and Chemical Biology, Harvard University, Cambridge, Massachusetts 02138, United States
- Daniel M. Hofmann School of Chemical Sciences, University of Illinois at Urbana-Champaign, Urbana, Illinois 61802, United States
- **Toby J. Woods** School of Chemical Sciences, University of Illinois at Urbana-Champaign, Urbana, Illinois 61802, United States; Oorcid.org/0000-0002-1737-811X

Complete contact information is available at:

https://pubs.acs.org/10.1021/jacs.3c05981

#### Notes

The authors declare no competing financial interest.

### ACKNOWLEDGMENTS

This work was supported by the U.S. Department of Energy, Office of Sciences, Office of Basic Energy Sciences, Chemical Sciences, Geosciences, and Biosciences Division under award number DOE DE-SC002. The authors acknowledge the use of facilities and instrumentation at School of Chemical Sciences and the Materials Research Laboratory Central Research Facilities, University of Illinois, partially supported by NSF through the University of Illinois Materials Research Science and Engineering Center DMR-1720633.

### REFERENCES

- (1) Stillings, L. L. Selenium. Economic and Environmental Geology And Prospects For the Future Supply: U.S. Geological Survey Professional Papers, Schulz, K. J.; Bradley, D. C.; Seal, R. R.; DeYoung, J. H., Eds.; 2017; pp Q1—Q55.
- (2) Kavlak, G.; Graedel, T. E. Global Anthropogenic Selenium Cycles for 1940-2010. *Resour. Conserv. Recycl.* **2013**, 73, 17–22.
- (3) Macy, J. M.; Michel, T. A.; Kirsch, D. G. Selenate Reduction by a Pseudomonas Species: A New Mode of Anaerobic Respiration. *FEMS Microbiol. Lett.* **1989**, *61*, 195–198.
- (4) Wells, M.; Stolz, J. F. Microbial Selenium Metabolism: A Brief History, Biogeochemistry and Ecophysiology. *FEMS Microbiol. Ecol.* **2020**, *96*, fiaa209.
- (5) Presser, T. S. The Kesterson Effect. Environ. Manage. 1994, 18, 437-454.
- (6) Maher, M. J.; Macy, J. M. Crystallization and Preliminary X-Ray Analysis of the Selenate Reductase from Thauera Selenatis. *Acta Crystallogr. D Biol. Crystallogr.* **2002**, *58*, 706–708.
- (7) Maher, M. J.; Santini, J.; Pickering, I. J.; Prince, R. C.; Macy, J. M.; George, G. N. X-Ray Absorption Spectroscopy of Selenate Reductase. *Inorg. Chem.* **2004**, *43*, 402–404.
- (8) Nancharaiah, Y. V.; Lens, P. N. L. Ecology and Biotechnology of Selenium-Respiring Bacteria. *Microbiol. Mol. Biol. Rev.* **2015**, *79*, 61–80.
- (9) Wells, M.; McGarry, J.; Gaye, M. M.; Basu, P.; Oremland, R. S.; Stolz, J. F. Respiratory Selenite Reductase from Bacillus Selenitireducens Strain MLS10. *J. Bacteriol.* **2019**, *201*, 10-1128.
- (10) Eswayah, A. S.; Smith, T. J.; Gardiner, P. H. E. Microbial Transformations of Selenium Species of Relevance to Bioremediation. *Appl. Environ. Microbiol.* **2016**, *82*, 4848–4859.
- (11) Borah, S. N.; Goswami, L.; Sen, S.; Sachan, D.; Sarma, H.; Montes, M.; Peralta-Videa, J. R.; Pakshirajan, K.; Narayan, M. Selenite Bioreduction and Biosynthesis of Selenium Nanoparticles by Bacillus Paramycoides SP3 Isolated from Coal Mine Overburden Leachate. *Environ. Pollut.* **2021**, 285, No. 117519.
- (12) Zhang, W.; Chen, Z.; Liu, H.; Zhang, L.; Gao, P.; Li, D. Biosynthesis and Structural Characteristics of Selenium Nanoparticles by Pseudomonas Alcaliphila. *Colloids Surf. B. Biointerfaces* **2011**, 88, 196–201.
- (13) Ali, I.; Shrivastava, V. Recent Advances in Technologies for Removal and Recovery of Selenium from (Waste)Water: A Systematic Review. *J. Environ. Manage.* **2021**, 294, No. 112926.
- (14) Murphy, A. P. Removal of Selenate from Water by Chemical Reduction. *Ind. Eng. Chem. Res.* 1988, 27, 187–191.
- (15) Wang, J. J.; Tessier, C.; Holm, R. H. Analogue Reaction Systems of Selenate Reductase. *Inorg. Chem.* **2006**, *45*, 2979–2988.
- (16) Youngblut, M. D.; Tsai, C. L.; Clark, I. C.; Carlson, H. K.; Maglaqui, A. P.; Gau-Pan, P. S.; Redford, S. A.; Wong, A.; Tainer, J. A.; Coates, J. D. Perchlorate Reductase Is Distinguished by Active Site Aromatic Gate Residues. *J. Biol. Chem.* **2016**, 291, 9190–9202.

- (17) Zheng, H.; Wisedchaisri, G.; Gonen, T. Crystal Structure of a Nitrate/Nitrite Exchanger. *Nature* **2013**, 497, 647–651.
- (18) Matson, E. M.; Park, Y. J.; Fout, A. R. Facile Nitrite Reduction in a Non-Heme Iron System: Formation of an Iron(III)-Oxo. *J. Am. Chem. Soc.* **2014**, *136*, 17398–17401.
- (19) Ford, C. L.; Park, Y. J.; Matson, E. M.; Gordon, Z.; Fout, A. R. A Bioinspired Iron Catalyst for Nitrate and Perchlorate Reduction. *Science* **2016**, *354*, 741–743.
- (20) Drummond, M. J.; Miller, T. J.; Ford, C. L.; Fout, A. R. Catalytic Perchlorate Reduction Using Iron: Mechanistic Insights and Improved Catalyst Turnover. ACS Catal. 2020, 10, 3175—3182.
- (21) Park, Y. J.; Peñas-Defrutos, M. N.; Drummond, M. J.; Gordon, Z.; Kelly, O. R.; Garvey, I. J.; Gullett, K. L.; García-Melchor, M.; Fout, A. R. Secondary Coordination Sphere Influences the Formation of Fe(III)-O or Fe(III)-OH in Nitrite Reduction: A Synthetic and Computational Study. *Inorg. Chem.* **2022**, *61*, 8182–8192.
- (22) MacBeth, C. E.; Golombek, A. P.; Young, J.; Yang, C.; Kuczera, K.; Hendrich, M. P.; Borovik, A. S. O2 Activation by Nonheme Iron Complexes: A Monomeric Fe(III)-Oxo Complex Derived from O2. *Science* **2000**, 289, 938–941.
- (23) Beckmann, U.; Süslüyan, D.; Kunz, P. C. Is the 1JPSe Coupling Constant a Reliable Probe for the Basicity of Phosphines? A 31P NMR Study. *Phosphorus, Sulfur Silicon Relat. Elem.* **2011**, *186*, 2061–2070.
- (24) Larsen, P. L.; Gupta, R.; Powell, D. R.; Borovik, A. S. Chalcogens as Terminal Ligands to Iron: Synthesis and Structure of Complexes with FeIII-S and FeIII-Se Motifs. *J. Am. Chem. Soc.* **2004**, *126*, 6522–6523.
- (25) Trans, D.; Addison, A. W.; Rao, T. N. Synthesis, Structure, and Spectroscopic Properties, 1984, No. 1.
- (26) Matson, E. M.; Bertke, J. A.; Fout, A. R. Isolation of Iron(II) Aqua and Hydroxyl Complexes Featuring a Tripodal H-Bond Donor and Acceptor Ligand. *Inorg. Chem.* **2014**, *53*, 4450–4458.
- (27) Fernández-Llamosas, H.; Castro, L.; Blázquez, M. L.; Díaz, E.; Carmona, M. Speeding up Bioproduction of Selenium Nanoparticles by Using Vibrio Natriegens as Microbial Factory. *Sci. Rep.* **2017**, *7*, No. 16046.
- (28) Hunter, W. J.; Manter, D. K. Reduction of Selenite to Elemental Red Selenium by Pseudomonas Sp. Strain CA5. *Curr. Microbiol.* **2009**, *58*, 493–498.
- (29) Młochowski, J.; Brząszcz, M.; Giurg, M.; Palus, J.; Wójtowicz, H. Selenium-Promoted Oxidation of Organic Compounds: Reactions and Mechanisms. *European J. Org. Chem.* **2003**, 2003, 4329–4339.
- (30) Młochowski, J.; Wójtowicz-Młochowska, H. Developments in Synthetic Application of Selenium(IV) Oxide and Organoselenium Compounds as Oxygen Donors and Oxygen-Transfer Agents. *Molecules.* **2015**, *20*, 10205–10243.